NASA Technical Memorandum 102490

Prediction of High Temperature Metal Matrix Composite Ply Properties

J.J. Caruso and C.C. Chamis
Lewis Research Center
Cleveland, Ohio

Presented at the
29th Structures, Structural Dynamics, and Materials (SDM) Conference
cosponsored by the AIAA, ASME, AHS, and ASC
Williamsburg, Virginia, April 18-20, 1988

NASA

PREDICTION OF HIGH TEMPERATURE METAL MATRIX COMPOSITE PLY PROPERTIES

J.J. Caruso and C.C. Chamis
National Aeronautics and Space Administration
Lewis Research Center
Cleveland, Ohio 44135

SUMMARY

The application of the finite element method (superelement technique) in conjunction with basic concepts from mechanics of materials theory is demonstrated to predict the thermomechanical behavior of high temperature metal matrix composites (HTMMC). The simulated behavior is used as a basis to establish characteristic properties of a unidirectional composite idealized as an equivalent homogeneous material. The ply properties predicted include: thermal properties (thermal conductivities and thermal expansion coefficients) and mechanical properties (moduli and Poisson's ratio). These properties are compared with those predicted by a simplified, analytical composite micromechanics model. This paper illustrates the predictive capabilities of the finite element method and the simplified model through the simulation of the thermomechanical behavior of a P100-graphite/copper unidirectional composite at room temperature and near matrix melting temperature. The advantage of the finite element analysis approach is its ability to more precisely represent the composite local geometry and hence capture the subtle effects that are dependent on this. The closed form micromechanics model does a good job at representing the average behavior of the constituents to predict composite behavior.

E-5280

INTRODUCTION

High temperature metal matrix composites (HTMMC) are emerging as candidate materials offering high potential payoffs in hot structures applications for advanced aerospace propulsion systems. Realization of these high potential payoffs depend on the development of: (1) fabrication techniques, (2) experimental techniques for characterizing the complex nonlinear behavior anticipated for these applications, and (3) computational methods for engineering design that account for this complex behavior.

Recent research at NASA Lewis Research Center has demonstrated two approaches for predicting HTMMC behavior. These approaches consist of: (1) application of the finite element method (superelement technique) in conjunction with concepts from mechanics of materials theory and (2) application of closed-form equations derived from a simplified, analytical micromechanics model. The first approach has previously been demonstrated by Caruso (ref. 1) and Caruso and Chamis (ref. 2) to predict equivalent thermal and mechanical properties of polymer matrix composites. The second approach employs a variation of the micromechanics model developed by Hopkins and Chamis (ref. 3) in a form more recently implemented by Hopkins and Murthy (ref. 4).

The objectives of this paper are to: (1) describe the application of the finite element method in conjunction with the mechanics of materials concepts as an approach to HTMMC micromechanical modeling and (2) compare the finite element results with those predictions based on the closed-form model implemented in the Metal Matrix Composite Analyzer (METCAN computer code) (ref. 4).

LIST OF SYMBOLS

A	area
dT	change in temperature
E	Young's modulus
F	force
G	shear modulus
K	thermal conductivity
L	length
q_t	flux
u	displacement
α	thermal expansion coefficient
ν	Poisson's ratio

Subscripts

x,y,z	denotes the components of the global structural Cartesian coordinate system
1,2,3	denotes the components of the composite material Cartesian coordinate system

MODEL DESCRIPTION

In the analytical micromechanics model, the representation of the fundamental unidirectional composite unit cell is a square array. The unit cell contains a single circular fiber surrounded by matrix to form a square array. In the finite element model, the representation is also a unit cell. The unit cell subsequently becomes the "superelement" that can be "imaged" to form the complete nine-cell model (fig. 1). The impetus for adapting the superelement technique is derived from: (1) the ability to represent a single square array (fiber/matrix unit cell) that could be easily modified, (2) the consistency with which the single unit cell can serve as the building block to form a multicell model with the ability thereby provided to create a stiffness matrix of the multicell model with much fewer total degrees of freedom compared to the full discretization, and (3) the capability to simulate multicell models substantially larger than conventional finite element analysis would allow. The superelement model (fig. 1) consists of one primary superelement (center cell) containing 192 three-dimensional solid (hexahedron and pentahedron) isoparametric elements and eight secondary or "image" superelements, comprising a total of 1133 grid points. The MSC/NASTRAN (ref. 5) general purpose finite element analysis software was used for the simulation. The load and boundary

conditions are applied to the model as enforced grid point displacements and/or temperatures.

The single cell is modeled in such a manner so as to allow the fiber volume ratio (FVR) to be varied to any one of the four values: 7, 22, 47, or 62 percent, rather routinely. This is achieved by changing the elements along the circumference of the fiber to matrix elements thereby decreasing the diameter of the fiber. As previously mentioned, the particular composite system chosen for the study consists of P100-graphite fiber (an orthotropic material) and a pure copper matrix (an isotropic material). Values of constituent properties at room (70 °F) and elevated (1500 °F) temperature assumed for the study are summarized in table I.

ANALYSIS PROCEDURE

The following sections describe the analysis procedures to determine the mechanical and thermal properties, which involves the choice of appropriate boundary and loading conditions together with the relevant equations from mechanics of materials concepts. Composite moduli are determined by obtaining forces from the finite element stress analysis resulting from prescribed displacements and calculating the property using the associated mechanics of materials equations. Likewise, composite Poisson's ratios and thermal expansions coefficients are calculated by obtaining the displacements from the finite element stress analysis which results from prescribed mechanical and thermal loading, respectively, again calculating the property using the associated mechanics of materials equations. The composite thermal conductivity is determined by obtaining the flux and free surface temperature from the finite element heat conduction analysis and calculating the composite property from thermodynamics concepts. The composite properties at elevated temperatures are predicted assuming steady state equilibrium conditions. Under these conditions, temperature dependent properties and linear analysis are considered to be adequate.

MECHANICAL PROPERTIES

The mechanical properties simulated from finite element analysis and the predictions of METCAN methods are described below. The properties are for room temperature (70 °F) and high temperature (1500 °F) conditions.

Longitudinal Modulus and Poisson's Ratio ($E_{\ell 11}$ and $\nu_{\ell 12}$)

The boundary and load conditions for the finite element simulation are applied to the composite through enforced displacements (including prescribed zero displacements). The boundary conditions are as follows:

(1) Constrain the degrees of freedom on the front YZ-plane in the X-direction (fig. 2).

(2) Constrain the degrees of freedom on the centerline parallel to the X-axis on the top and bottom XY-planes in the Y-direction.

(3) Constrain the degrees of freedom on the centerline parallel to the X-axis on the right and left XZ-planes in the Z-direction.

The composite is loaded with a prescribed uniform displacement on the back YZ-plane in the X-direction.

The composite longitudinal modulus is calculated from the following equation:

$$E_{\ell 11} = \frac{\sigma_{\ell 11}}{\varepsilon_{\ell 11}}$$

where $\sigma_{\ell 11}$ is the applied stress due to an enforced displacement on the YZ face and $\varepsilon_{\ell 11}$ is the longitudinal strain.

The longitudinal modulus simulated by the finite element analysis is plotted as a function of fiber volume ratio (FVR) for the room and high temperature conditions in figure 3. The METCAN predictions are plotted for comparison purposes in figure 3. The comparison between the two results is, as expected, very good.

The longitudinal Poisson's ratio is calculated from the following equation:

$$\nu_{\ell 12} = \frac{\varepsilon_{\ell 22}}{\varepsilon_{\ell 11}}$$

where $\varepsilon_{\ell 11}$ is the longitudinal strain in the load direction and $\varepsilon_{\ell 22}$ is the transverse strain in the unloaded direction.

Poisson's ratio as predicted by the finite element simulation shows little effect to temperature (fig. 4). Poisson's ratio is affected by neighboring fibers and the multicell finite element results show this when compared to the METCAN predicted result which does not take this affect into account. The affect of other fibers on Poisson's ratio represents a displacement compatibility (due to Poisson effects) between the cells which is not considered for the single cell model or METCAN. The METCAN prediction becomes worse as the FVR increases. This is because as the FVR increases the displacement incompatibility becomes more predominant; however, the trend is in the same direction.

Transverse Modulus and Poisson's Ratio ($E_{\ell 22}$ and $\nu_{\ell 23}$)

The boundary and load conditions for the finite element simulation are applied through enforced displacements (including prescribed zero displacements). The boundary conditions are as follows:

(1) Constrain the degrees of freedom in the center YZ-plane in the X-direction (fig. 2).

(2) Constrain the degrees of freedom in the bottom XY-plane in the Z-direction.

(3) Constrain the degrees of freedom on the centerline parallel to the X-axis on the top and bottom XY-plane in the Y-direction.

The composite is loaded with a prescribed displacement on the top XY-plane in the Z-direction.

The transverse modulus is calculated from the following equation:

$$E_{\ell 33} = \frac{\sigma_{\ell 33}}{\varepsilon_{\ell 33}}$$

where $\sigma_{\ell 33}$ is the applied stress due to an enforced displacement on the YZ face and $\varepsilon_{\ell 33}$ is the longitudinal strain.

As shown in figure 5, the modulus decreases with increasing FVR. This is expected because the transverse modulus of the matrix is larger than that of the fiber. The METCAN predictions (the continuous curves) are practically identical with the finite element simulations at both temperatures but deviate slightly with decreasing FVR.

The transverse Poisson's ratio is calculated from the following equation:

$$\nu_{\ell 23} = \frac{\varepsilon_{\ell 22}}{\varepsilon_{\ell 33}}$$

where $\sigma_{\ell 33}$ is the transverse strain in the load direction and $\varepsilon_{\ell 22}$ is the transverse strain in the unloaded direction.

Poisson's ratio as predicted by the finite element simulation shows little effect to temperature (fig. 6). The Poisson's ratio ($\nu_{\ell 23}$) is greatly affected by the neighboring fibers and the multicell finite element results show this when compared to the METCAN results which do not take this affect into account. Values for $\nu_{\ell 23}$ are plotted assuming transverse isotropy (curves labeled isotropic) for comparison to the two methods described here. That is the transversely isotropic relation between $\nu_{\ell 23}$, $G_{\ell 23}$, and $E_{\ell 22}\left(\nu_{\ell 23} = \frac{E_{\ell 22}}{2G_{\ell 23}} - 1\right)$ may not be justified on the constituent level.

Shear Modulus $G_{\ell 12}$

The boundary and load conditions for the finite element simulation are applied through enforced displacements (including prescribed zero displacements). The boundary conditions are as follows:

(1) Constrain the degrees of freedom in the left XZ-plane in the X-direction (fig. 2).

(2) Constrain the degrees of freedom for all nodes in the Y- and Z-direction.

The composite has a prescribed displacement on the right XZ-plane in the X-direction.

The modulus is calculated from the following equation:

$$G_{\ell 12} = \frac{\tau_{\ell 12}}{\gamma_{\ell 12}}$$

where $\tau_{\ell 12}$ is the applied stress due to an enforced displacement on the XZ face and $\gamma_{\ell 12}$ is the transverse strain.

The finite element predictions (fig. 7) show the high temperature property is smaller than the room temperature property. This is expected since at high temperature P100 and copper have lower shear moduli than at room temperature. The METCAN predictions (continuous curve) compare well with the finite element prediction at both temperatures through the full range of FVR. These results further indicate that adjacent fibers have negligible influence on the shear modulus.

Shear Modulus $G_{\ell 23}$

The boundary and load conditions for the finite element analysis are applied through enforced displacements (including prescribed zero displacements). The boundary conditions are as follows:

(1) Constrain the degrees of freedom in the left XZ-plane in the Z-direction (fig. 2).

(2) Constrain the degrees of freedom for all nodes in the X- and Y-direction.

The composite has a prescribed displacement on the right XZ-plane in the Z-direction.

The modulus is calculated from the following equation:

$$G_{\ell 23} = \frac{\tau_{\ell 23}}{\gamma_{\ell 23}}$$

where $\tau_{\ell 23}$ is the applied stress due to an enforced displacement on the XZ face and $\gamma_{\ell 23}$ is the transverse strain.

The finite element predictions for $G_{\ell 23}$ are similar to those for $G_{\ell 12}$ (fig. 8). The METCAN predictions (continuous curve) are in good agreement with those from the finite element method at both temperatures through all FVR.

THERMAL PROPERTIES

The thermal properties synthesized from the finite element simulation and those predicted by the simplified micromechanics model implemented in METCAN are described below. The properties are for both room temperature (70 °F) and high temperature (1500 °F) conditions. The thermal properties of interest include expansion coefficients and conductivities.

Longitudinal and Transverse Thermal Expansion Coefficient

The boundary and load conditions for the finite element analysis are applied through enforced displacements (including prescribed zero displacements) and temperatures. The boundary conditions are as follows:

(1) Constrain the degrees of freedom on the center YZ-plane in the X-direction (fig. 2).

(2) Constrain the degrees of freedom on the centerline parallel to the X-axis on the top and bottom XY-plane in the Y-direction.

(3) Constrain the degrees of freedom on the centerline parallel to the X-axis on the right and left XZ-plane in the Z-direction.

The composite is subject to a uniform temperature applied to the entire structure.

The thermal expansion coefficients are calculated from the following equations:

$$\alpha_{\ell 11} = \frac{\varepsilon_{\ell 11}}{\nabla T}$$

$$\alpha_{\ell 22} = \frac{\varepsilon_{\ell 22}}{\nabla T}$$

where $\varepsilon_{\ell 11}$ is the longitudinal strain, $\varepsilon_{\ell 22}$ is the transverse strain and ∇T is the temperature change.

The longitudinal expansion as shown in figure 9 decreases rapidly with increasing FVR. This large decrease is due primarily to the negative expansion coefficient of the P100. The METCAN predictions (continuous curve) are in good agreement with and follow the same trend as the finite element predictions through all FVR.

The finite element predictions for the transverse expansion (fig. 10) are affected by the neighboring fibers. The expansion coefficient increases slightly with increasing FVR up to about 0.4 and then the decrease slightly with increasing FVR greater than 0.4. This occurs at high temperature and room temperature. The METCAN predictions follow the same general trend as the super-element predictions at room and high temperature for all FVR. The room temperature METCAN prediction (continuous curve) is in better agreement than the high temperature prediction although both are considered reasonable based on the simplified assumptions in METCAN.

Longitudinal Thermal Conductivity

The boundary and load conditions for the finite element analysis are applied through enforced temperatures. The boundary conditions are as follows:

(1) Constrain the temperature of the atmosphere (fig. 2) on the cold face (front YZ-plane) to 0 °F.

(2) Insulate the structure on the four sides parallel to the heat flow.

(3) Constrain the back YZ-plane to conduct heat to the atmosphere.

The composite is subject to an increase in temperature to the front YZ-plane.

The longitudinal thermal conductivity is calculated from the following equations:

$$K_{\ell 11} = \frac{q_t \cdot L_x}{A \cdot \nabla T}$$

where, q_t is the flux through the composite, L_x is the X length, A is the cross-sectional area, and ∇T is the temperature change.

The finite element and METCAN predictions of the longitudinal conductivity are shown in figure 11. The room and high temperature predictions increase with increasing FVR. The room temperature METCAN predictions are slightly lower than the finite element prediction while the high temperature METCAN predictions are slightly higher than the superelement predictions.

Transverse Thermal Conductivity

The boundary and load conditions for the finite element analysis are applied through enforced temperatures. The boundary conditions are as follows:

(1) Constrain the temperature of the atmosphere (fig. 2) on the cold face (right XZ-plane) to 0 °F.

(2) Insulate the structure on the four sides parallel to the heat flow.

(3) Constrain the left XZ-plane to conduct heat to the atmosphere.

The composite is subject to an increase in temperature to the right YZ-plane.

The transverse thermal conductivity is calculated from the following equations:

$$K_{\ell 22} = \frac{q_t \cdot L_y}{A \cdot \nabla T}$$

where, q_t is the flux through the composite, L_y is the Y width, A is the cross-sectional area, and ∇T is the temperature change.

The finite element and METCAN predictions are shown in figure 12 for the transverse thermal conductivity. The predictions decrease with increasing FVR for room and high temperature. The METCAN results are lower than the finite element predictions for both room and high temperature. Since the finite element predictions are higher at low FVR and approach the METCAN results as the FVR is increased, it may be concluded that denser whiskers may be required for smaller diameter fibers.

SUMMARY OF RESULTS

The important results of adapting mechanics of materials concepts with finite element analysis, or alternatively the simplified analytical models such as is implemented in METCAN, to HTMMC micromechanics are as follows:

(1) The mechanics of materials concepts and the finite element (superelement) method provides an independent method of predicting the thermomechanical properties of MMC at room and high temperature.

(2) The mechanical properties include moduli and Poisson's ratio. Comparisons with the simplified micromechanics equations (METCAN) are in good agreement. Poisson's ratio ($\nu_{\ell 23}$) does not satisfy the assumption of transverse isotropy.

(3) The thermal properties include thermal expansion coefficients and thermal heat conductivities. The longitudinal thermal expansion coefficient predicted by METCAN is in good agreement with the finite element results. The transverse thermal expansion coefficient predicted by METCAN deviates slightly from the finite element results. The thermal conductivities predicted from METCAN are in good agreement with the finite element simulations.

CONCLUSION

The important conclusions of adapting the superelement method to thermomechanical behavior of HTMMC are as follows:

1. The finite element technique used in conjunction with mechanics of materials concepts provides the ability to analyze ordinary composite structures well and offers an alternative for predicting composite properties. Because of its utility this method can be extended to analyze more complex composite interactions. These may include fiber fracture, fiber/matrix disbonding, hybrid composites, etc.

2. The superelement method can provide detailed information about local composite behavior that cannot be obtained through experiments.

REFERENCES

1. Caruso, J.J., "Application of Finite Element Substructuring to Composite Micromechanics," NASA TM-83729, 1984.

2. Caruso, J.J. and Chamis, C.C., "Assessment of Simplified Composite Micromechanics Using Three-Dimensional Finite-Element Analysis," Journal of Composites Technology and Research, Vol. 2, No. 3, Fall 1986, pp. 77-83.

3. Hopkins, D.A. and Chamis, C.C., "Simplified Composite Micromechanics Equations for Hygral, Thermal and Mechanical Properties," NASA TM-83320, 1983.

4. Hopkins, D.A. and Murthy, P.L.N., "METCAN - the Metal Matrix Composite Analyzer," Lewis Structures Technology 1988, Vol. 2, Structural Mechanics, NASA CP-3003-VOL-2, 1988, pp. 141-156.

5. Schaeffer H.G., MSC/NASTRAN: Primer Static and Normal Modes Analysis, Schaeffer Analysis, Inc., 1979.

TABLE I. - FIBER AND MATRIX PROPERTIES

Property symbol	Units	Temperature, °F			
		70		1500	
		P100	Copper	P100	Copper
Longitudinal modulus	E_{11} Mpsi	105.0	17.0	93.8	8.87
Transverse modulus	E_{22} Mpsi	.90	17.0	.804	8.87
Longitudinal shear mosulus	G_{12} Mpsi	1.10	6.54	.982	3.41
Transverse shear modulus	G_{23} Mpsi	.70	6.45	.625	3.41
Longitudinal Poisson's ratio	ν_{12}	.200	.300	.179	.300
Transverse Poisson's ratio	ν_{23}	.250	.300	.223	.300
Longitudinal heat conduction	K_{11} $\frac{\text{Btu in.}}{\text{hr °F in.}^2}$	25.	19.3	24.4	16.8
Transverse heat conduction	K_{22} $\frac{\text{Btu in.}}{\text{hr °F in.}^2}$	1.74	19.3	1.70	16.8
Longitudinal thermal expansion	α_{11} $\times 10^{-6}$ $\frac{\text{in.}}{\text{in. °F}}$	-.90	9.8	-1.01	19.6
Transverse thermal expansion	α_{22} $\times 10^{-6}$ $\frac{\text{in.}}{\text{in. °F}}$	5.6	9.8	6.27	19.6

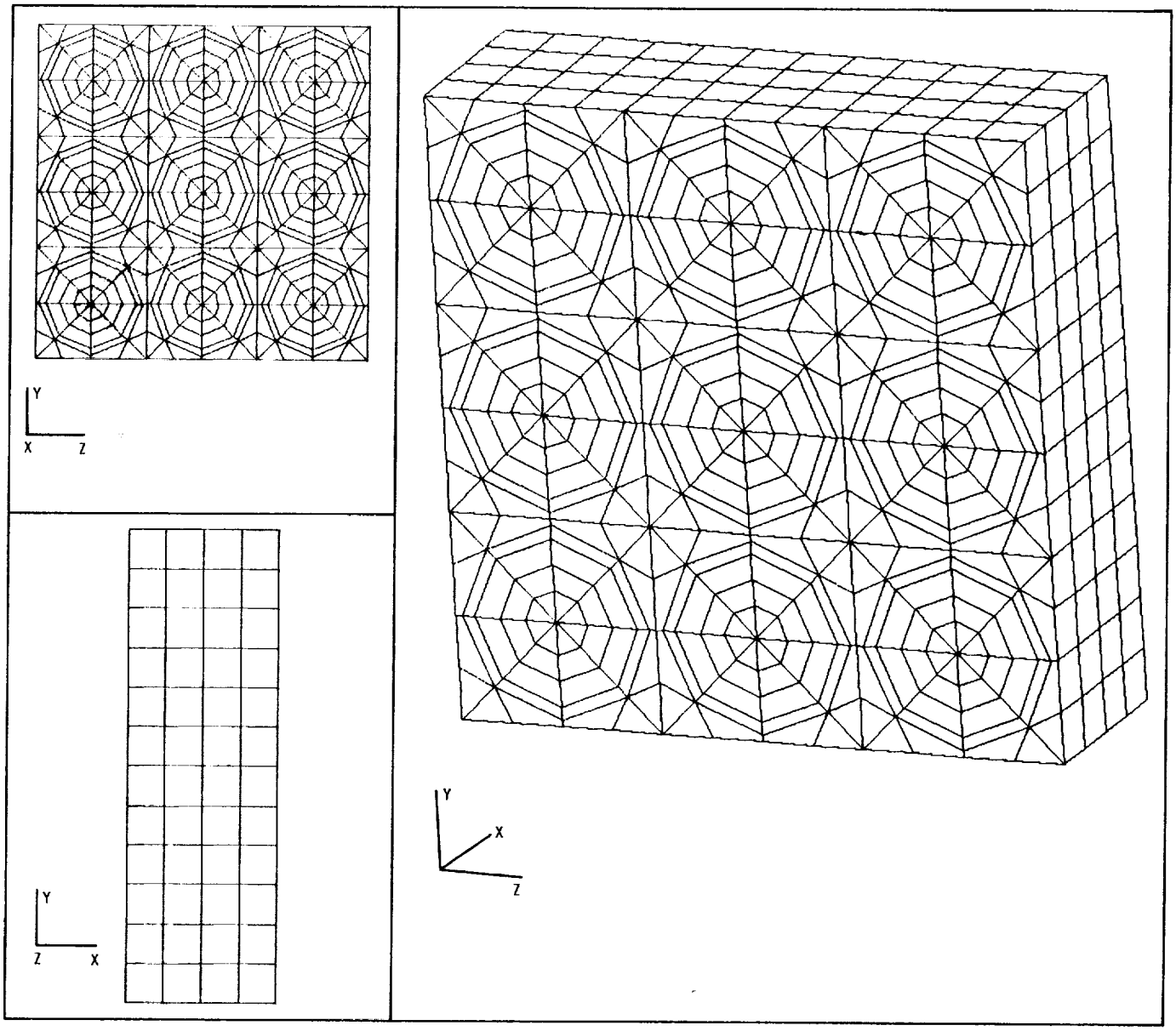

FIGURE 1. - 9-CELL FINITE ELEMENT MODEL.

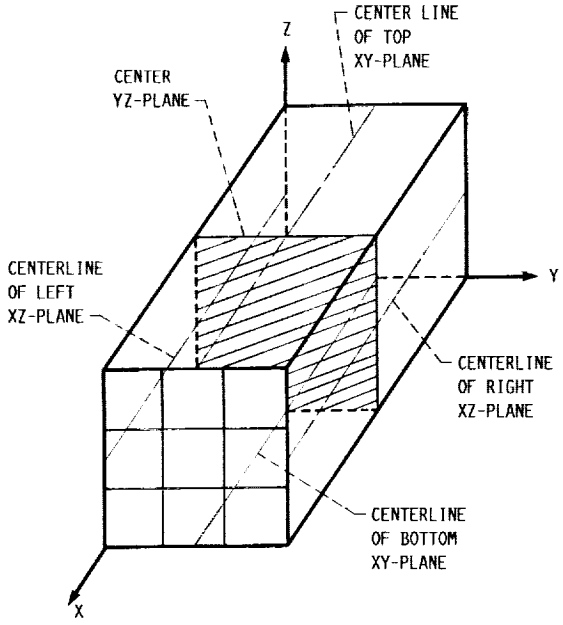

FIGURE 2. - GENERAL BOUNDARY CONDITIONS FOR THE 3-D SUPER-ELEMENT MODEL.

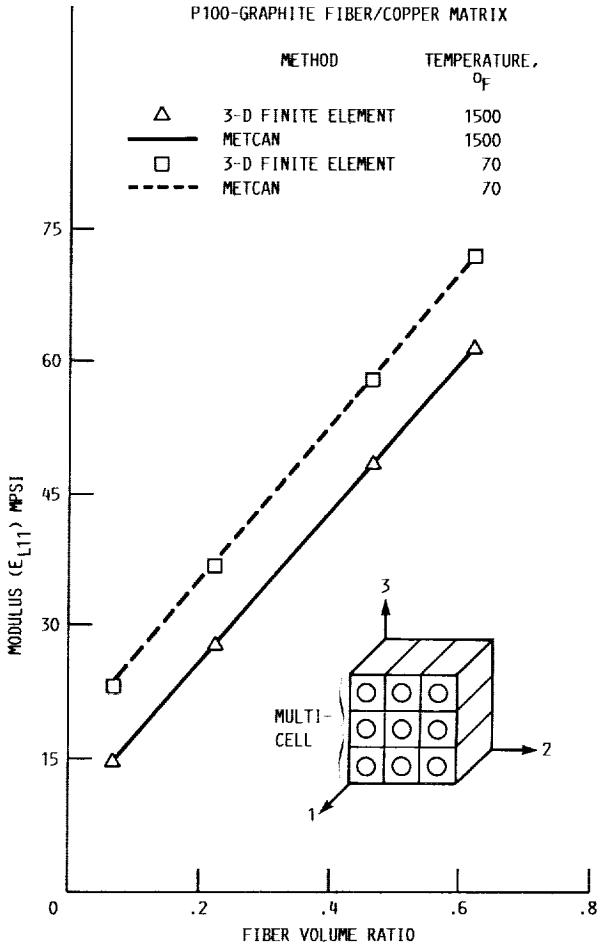

FIGURE 3. - LONGITUDINAL MODULUS OF UNIDIRECTIONAL COMPOSITES.

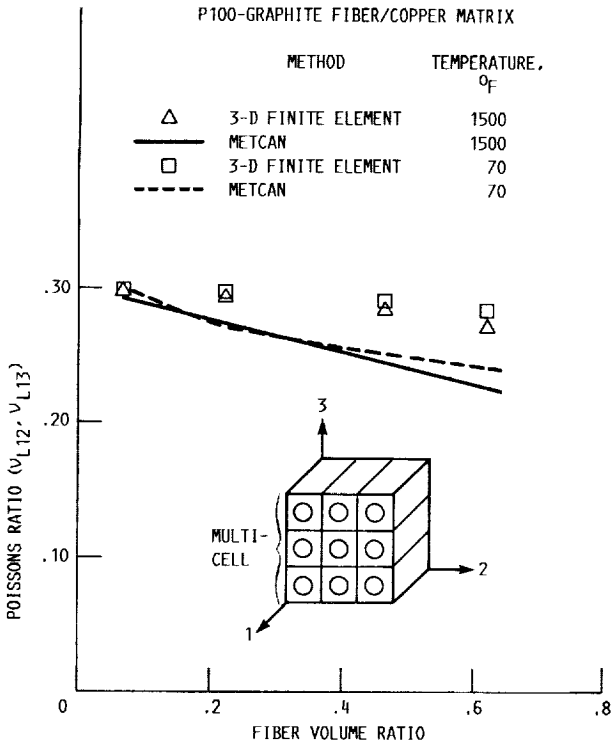

FIGURE 4. - POISSONS RATIO OF UNIDIRECTIONAL COMPOSITES.

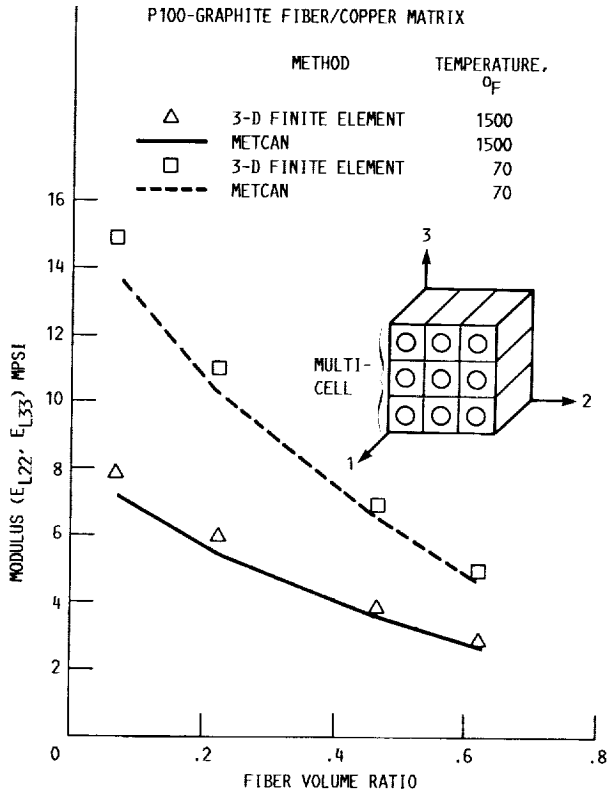

FIGURE 5. - TRANSVERSE MODULUS OF UNIDIRECTIONAL COMPOSITES.

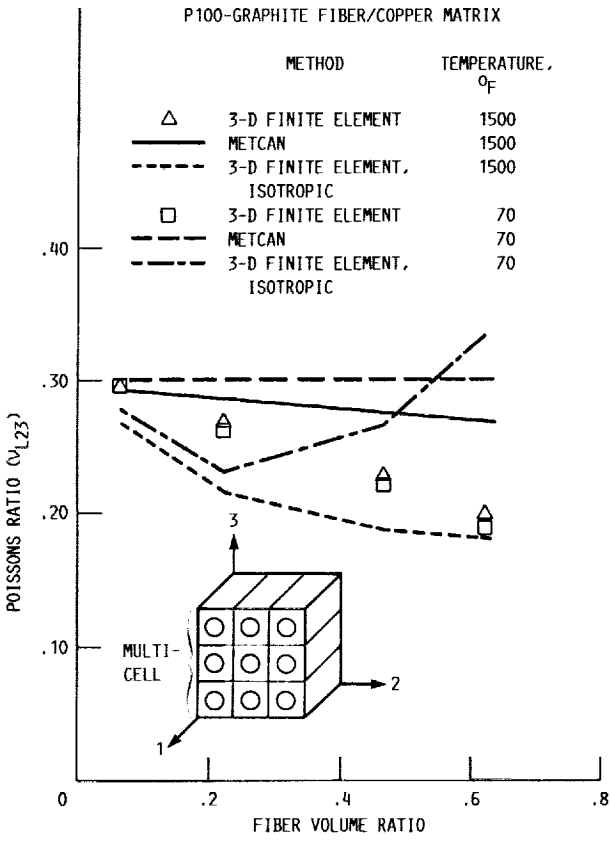

FIGURE 6. - POISSONS RATIO OF UNIDIRECTIONAL COMPOSITES.

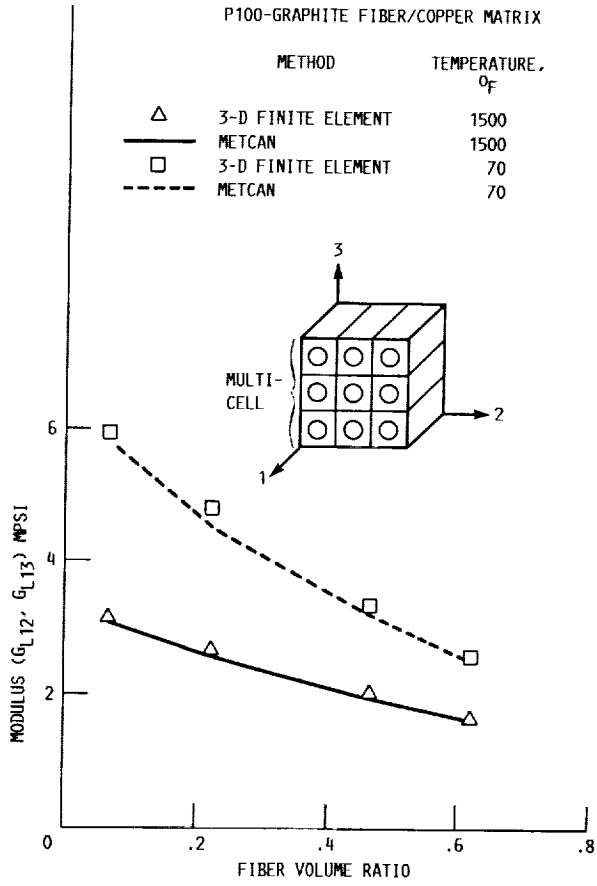

FIGURE 7. - SHEAR MODULUS OF UNIDIRECTIONAL COMPOSITES.

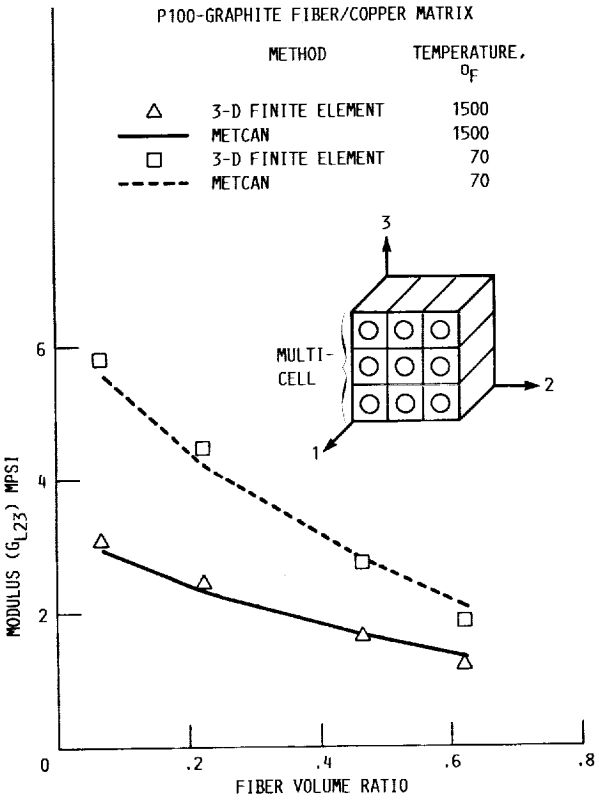

FIGURE 8. - SHEAR MODULUS OF UNIDIRECTIONAL COMPOSITES.

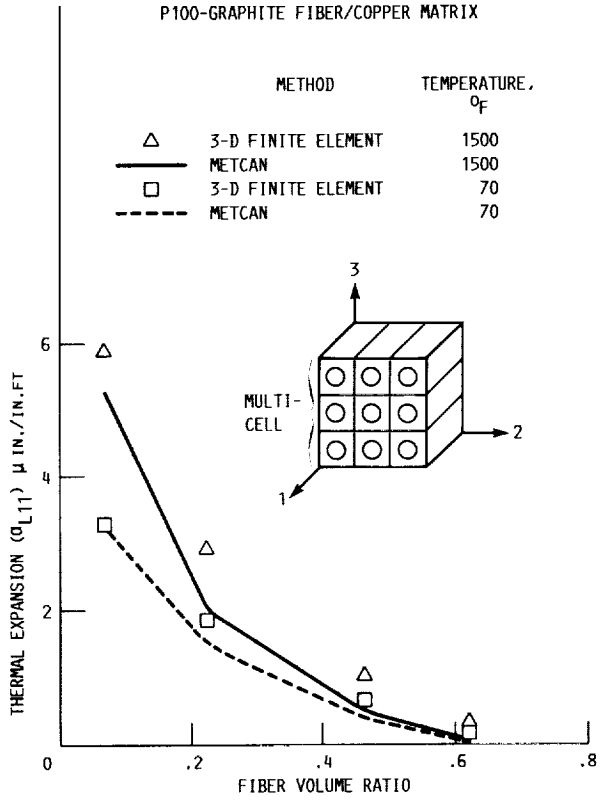

FIGURE 9. - LONGITUDINAL THERMAL EXPANSION OF UNIDIRECTIONAL COMPOSITES.

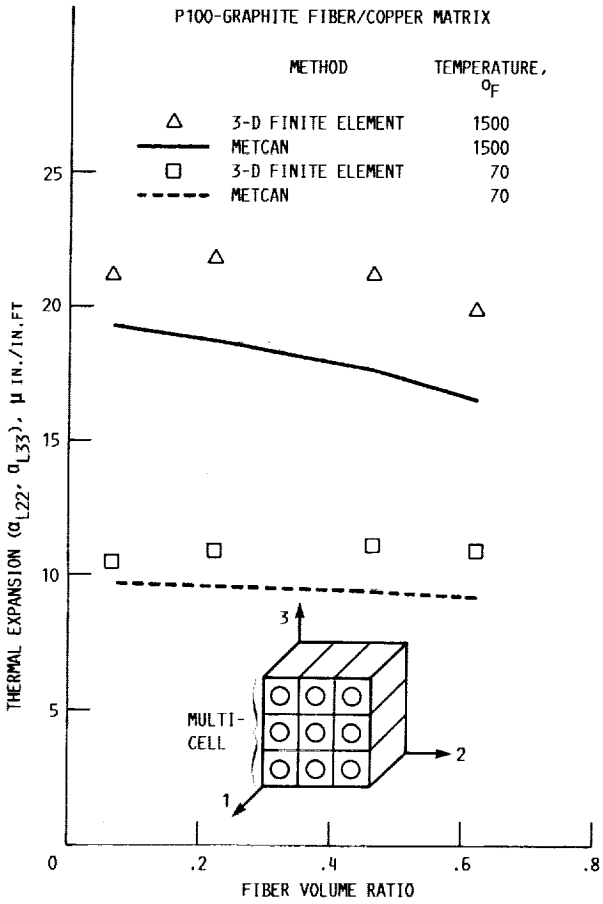

FIGURE 10. - TRANSVERSE THERMAL EXPANSION OF UNIDIRECTIONAL COMPOSITES.

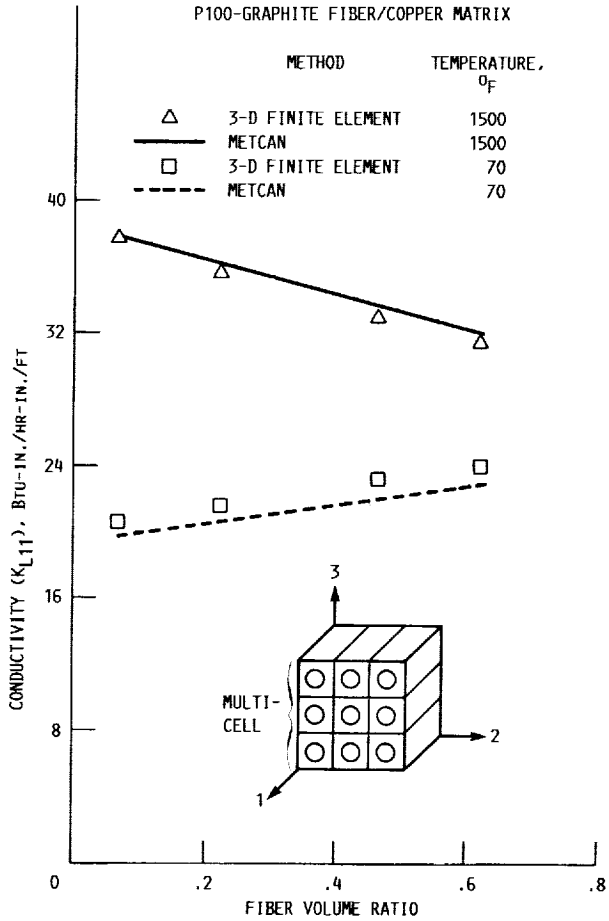

FIGURE 11. - LONGITUDINAL THERMAL CONDUCTIVITY OF UNIDIRECTIONAL COMPOSITES.

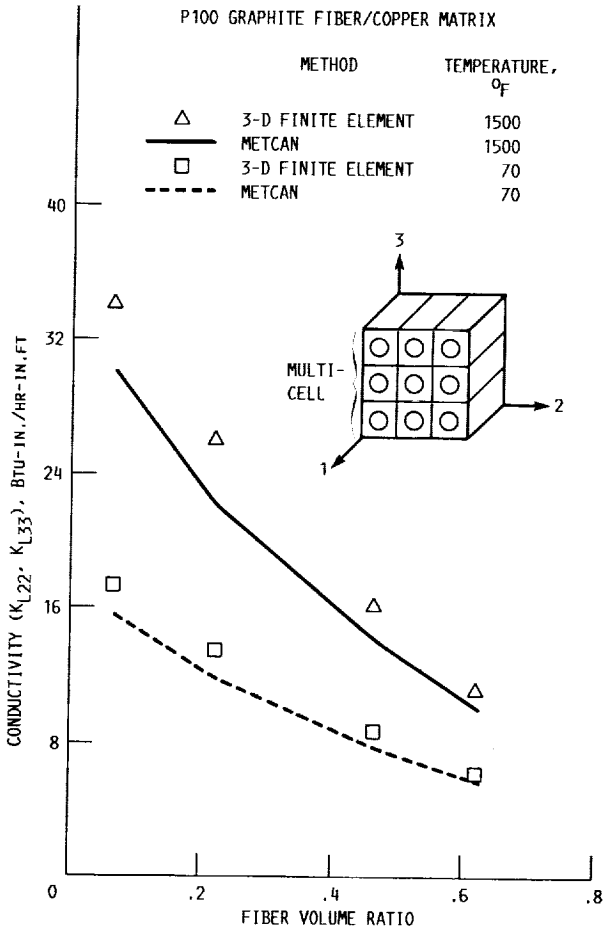

FIGURE 12. - TRANSVERSE THERMAL CONDUCTIVITY OF UNI-DIRECTIONAL COMPOSITES.

NASA
National Aeronautics and Space Administration

Report Documentation Page

1. Report No.	2. Government Accession No.	3. Recipient's Catalog No.
NASA TM-102490		

4. Title and Subtitle	5. Report Date
Prediction of High Temperature Metal Matrix Composite Ply Properties	6. Performing Organization Code

7. Author(s)	8. Performing Organization Report No.
J.J. Caruso and C.C. Chamis	E-5280
	10. Work Unit No. 505-63-11

9. Performing Organization Name and Address	11. Contract or Grant No.
National Aeronautics and Space Administration Lewis Research Center Cleveland, Ohio 44135-3191	13. Type of Report and Period Covered Technical Memorandum

12. Sponsoring Agency Name and Address	14. Sponsoring Agency Code
National Aeronautics and Space Administration Washington, D.C. 20546-0001	

15. Supplementary Notes

Presented at the 29th Structures, Structural Dynamics, and Materials (SDM) Conference cosponsored by the AIAA, ASME, AHS, and ASC, Williamsburg, Virginia, April 18-20, 1988.

16. Abstract

The application of the finite element method (superelement technique) in conjunction with basic concepts from mechanics of materials theory is demonstrated to predict the thermomechanical behavior of high temperature metal matrix composites (HTMMC). The simulated behavior is used as a basis to establish characteristic properties of a unidirectional composite idealized as an equivalent homogeneous material. The ply properties predicted include: thermal properties (thermal conductivities and thermal expansion coefficients) and mechanical properties (moduli and Poisson's ratio). These properties are compared with those predicted by a simplified, analytical composite micromechanics model. This paper illustrates the predictive capabilities of the finite element method and the simplified model through the simulation of the thermomechanical behavior of a P100-graphite/copper unidirectional composite at room temperature and near matrix melting temperature. The advantage of the finite element analysis approach is its ability to more precisely represent the composite local geometry and hence capture the subtle effects that are dependent on this. The closed form micromechanics model does a good job at representing the average behavior of the constituents to predict composite behavior.

17. Key Words (Suggested by Author(s))	18. Distribution Statement
Composite properties; Metal matrix composites; High temperature metal matrix composites; Composites micromechanics; Finite element methods; Square array; Composite modulus; Composite Poisson's ratio; Composite thermal expansion; Composite thermal conductivity; P-100—graphite/copper	Unclassified – Unlimited Subject Category 24

19. Security Classif. (of this report)	20. Security Classif. (of this page)	21. No. of pages	22. Price*
Unclassified	Unclassified	12	A03

NASA FORM 1626 OCT 86

*For sale by the National Technical Information Service, Springfield, Virginia 22161